


Cite this: *RSC Adv.*, 2022, 12, 8804

# A magnetic porous organic polymer: catalytic application in the synthesis of hybrid pyridines with indole, triazole and sulfonamide moieties†

Morteza Torabi,<sup>a</sup> Meysam Yarie,<sup>ID</sup> <sup>\*a</sup> Mohammad Ali Zolfigol,<sup>ID</sup> <sup>\*a</sup> Saeid Azizian<sup>b</sup> and Yanlong Gu<sup>ID</sup> <sup>c</sup>

Herein, the synthesis and characterization of a triazine-based magnetic ionic porous organic polymer are reported. The structure, morphology, and components of the prepared structure have been investigated with several spectroscopic and microscopic techniques such as FT-IR, EDX, elemental mapping, TGA/DTA, SEM, TEM, VSM, and BET analysis. Also, catalytic application of the prepared triazine-based magnetic ionic porous organic polymer was investigated for the synthesis of hybrid pyridine derivatives bearing indole, triazole and sulfonamide groups. Furthermore, the prepared hybrid pyridine systems were characterized by FT-IR, <sup>1</sup>H NMR, <sup>13</sup>C NMR and mass analysis. A cooperative vinylogous anomeric-based oxidation pathway was suggested for the synthesis of target molecules.

Received 21st January 2022  
Accepted 7th March 2022

DOI: 10.1039/d2ra00451h

rsc.li/rsc-advances

## Introduction

Porous organic polymers (POPs) are a prominent category of porous solid materials.<sup>1–3</sup> Due to having unique properties such as tailored pore structures, high surface area, tunability of pores, designability, absolutely organic scaffold and excellent thermal stability, these series of compounds have a significant role in the advancement of science and technology.<sup>4–6</sup> In recent years, the innumerable applications of POPs have been palpable. High ability in gas storage and gas separation, catalytic applications, ion exchange, electrochemical energy storage, sensors, carriers, biomedicine, and optoelectronics are a few examples of POP applications.<sup>6,7</sup> Based on extensive synthetic routes, POPs are divided into different categories. These compounds include covalent organic frameworks (COFs), ionic porous organic polymers (IPOP), polymers of intrinsic microporosity (PIMs), conjugated microporous polymers (CMPs), hypercrosslinked polymers (HCPs) *etc.*<sup>8,9</sup> In recent years, ionic porous organic polymers (IPOP) as one of the novel types of POPs played an essential role in the areas of gas storage, separation, catalysis and chemosensors.<sup>10,11</sup> These materials have high charge density and acquired fantastic properties by incorporating charged groups into porous networks and the

counter anions can be changed for different goals. It is not an exaggeration to say, IPOP have created a bridge between ionic liquids and porous polymers.<sup>12,13</sup>

Generally, catalytic applications of POPs can be emerged by ionic, organo-catalytic, acidic/basic groups, chiral and organic ligands.<sup>14</sup> Specifically, IPOP with good designability, high specific surface area, easy accessibility, reusability, simple ion exchange and the durable active site can be converted to irreplaceable heterogeneous catalysts.<sup>15</sup> Some of the catalytic applications of IPOP include CO<sub>2</sub> fixation, Suzuki cross-coupling, oxidation and reduction reactions and phase transfer catalysis.<sup>10</sup>

Recently, magnetic ionic liquids as a subset of ionic liquids have been considered by many researchers and many applications have been developed for them.<sup>16–18</sup> However, magnetic ionic porous organic polymers (TMIPPOP) are less known and deserve more attention and can pave the way for new research lines in the areas of porous materials.

Pyridine scaffolds as the privileged heterocyclic nucleus have been found in many natural products, pharmaceutical active molecules, organic synthesis, supramolecular chemistry, functional materials, agricultural applications, coordination chemistry and catalytic systems.<sup>19–23</sup> These special systems have a vital role in biologically active natural substances such as nicotine, vitamin B6 and oxido-reductive NADP-NADPH coenzymes.<sup>24,25</sup> The irreplaceable properties of pyridine families as HIV protease inhibitor,<sup>26</sup> anticancer,<sup>27</sup> acetylcholinesterase inhibitor,<sup>24</sup> anti-inflammatory,<sup>28</sup> antihypertensive<sup>29</sup> and antidepressant<sup>30</sup> can be a persuasive reason for the synthesis of a new series of these compounds. As a sequence, sophisticated motifs of pyridine hybrids with several important organic groups are robust tools for drug design that significantly has attracted the attention of many industrial and academic scientists.<sup>31,32</sup>

<sup>a</sup>Department of Organic Chemistry, Faculty of Chemistry, Bu-Ali Sina University, Hamedan, Iran. E-mail: myari.5266@gmail.com; zolfigol@basu.ac.ir; mzolfigol@yahoo.com; Fax: +988138380709; Tel: +988138282807

<sup>b</sup>Department of Physical Chemistry, Faculty of Chemistry, Bu-Ali Sina University, Hamedan, Iran

<sup>c</sup>School of Chemistry and Chemical Engineering, Huazhong University of Science and Technology, 1037 Luoyu road, Hongshan District, Wuhan 430074, China

† Electronic supplementary information (ESI) available. See DOI: 10.1039/d2ra00451h



Sulfonamides have been introduced as the major family of organosulfur compounds.<sup>33–36</sup> Therefore, these compounds with exceptional advantages including high stability, three-dimensional shape, hydrophilic properties, favorable physico-chemical properties and having incomparable potential in modern antibiotics have revolutionized the areas of medicinal chemistry.<sup>36,37</sup> Sulfonamide families have special antibacterial properties and were introduced as highly important antimicrobials.<sup>38</sup> Furthermore, the privileged properties of sulfa drug as anti-bacterial,<sup>39</sup> anti-fungal,<sup>40</sup> HIV protease inhibitory,<sup>41</sup> anti-inflammatory,<sup>42</sup> anti-protozoal,<sup>43</sup> are well known.

On the other hand, triazole families are ubiquitous in many research fields such as drugs, dyes, chemosensors, metal complexes, organocatalysts and energetic materials.<sup>44–50</sup> Characteristically, 1,2,3-triazoles are unique scaffolds that are founded in numerous drugs and biologically active molecules such as xanthine oxidase inhibitors, c-Met kinase and have many applications as anti-microbial, anti-bacterial, anti-malarial, and other anti-cancer agents.<sup>51,52</sup> In particular, different hybrid structures of triazoles such as pyridine-triazole, indole-triazole and sulfonamide-triazole have fantastic properties as anti-cancer,<sup>53</sup> antimalarial,<sup>54</sup> anti-adipogenic,<sup>55</sup> anti-dyslipidemic<sup>55</sup> and anti-proliferative agents.<sup>56</sup> However, the agglomeration of several fundamental groups in a single molecule is very interesting and practical research. In this investigation, we applied a triazine-based magnetic ionic porous organic polymer (TMIPOP) as a catalyst for the synthesis of new series of heterocycles bearing four pharmacophore groups (pyridine, triazole, sulfonamide and indole) in a single molecule *via* a vinylogous anomeric based-oxidation<sup>57–59</sup> using multicomponent reaction strategy<sup>60–62</sup> (Schemes 1–3).

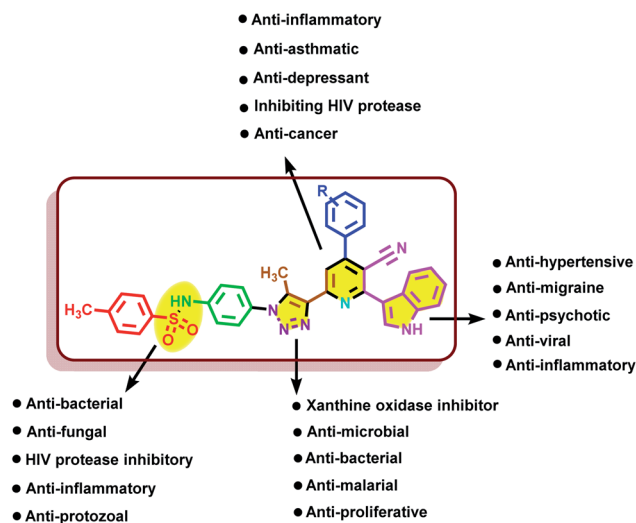
## Results and discussion

Several techniques such as FT-IR, EDX, elemental mapping, TGA/DTA, SEM, TEM, VSM, N<sub>2</sub> adsorption/desorption were used for the characterization of TMIPOP.

FT-IR spectra of TMIPOP, TIPOP and FeCl<sub>3</sub> are illustrated in Fig. 1. In the FT-IR spectrum of TIPOP, a broad pick at 3389 cm<sup>−1</sup> is related to the adsorbed moisture during the reaction. The diagnostic peak at 1590 cm<sup>−1</sup> is a typical stretching bond of C–N in DABCO. Also, a characteristic peak at 1054 cm<sup>−1</sup> described the stretching band of C–N in ammonium salt after completing of reaction. The related peak of triazine moiety is at 784 cm<sup>−1</sup>. The addition of FeCl<sub>3</sub> to TIPOP for the synthesis of TMIPOP leads to slight differences in the FT-IR spectrum which confirms the successful formation of the catalyst.

The magnetic susceptibility of TMIPOP was examined by VSM analysis. The magnetic moment of TMIPOP was measured in the magnetic field range of −10 000 to 10 000 Oe. According to the result, TMIPOP has a linear response to the magnetic field and magnetic susceptibility is 0.41 emu g<sup>−1</sup> (see ESI†).

The porous structure and specific surface area of TIPOP (A) and TMIPOP (B) were investigated using N<sub>2</sub> adsorption-desorption and the obtained data were shown in Fig. 2. TIPOP has a BET surface area of 18.59 m<sup>2</sup> g<sup>−1</sup>. Due to having polar and



Scheme 1 Co-existence of four pharmacophore groups within the structure of synthesized molecules.

cationic structure and ideal ability in water capturing the TIPOP does not have high porosity.<sup>5</sup> Furthermore, because of the N-rich structure of TIPOP, the interactions between N<sub>2</sub> gas and TIPOP are weak which leads to a decrease in N<sub>2</sub> adsorption (Fig. 2(A)). After adding FeCl<sub>3</sub> to TIPOP for magnetization of this polymer, the specific surface area of TMIPOP is reduced to 6.1 m<sup>2</sup> g<sup>−1</sup> indicating the FeCl<sub>3</sub> particles are located in the cavities of the polymer which leads to a decrease in the surface area compared to TIPOP (Fig. 2(B)).

The crystal structure of TIPOP and TMIPOP was investigated by XRD techniques (see ESI†). According to the XRD pattern of TIPOP the low angle peak (<10°) confirms the presence of mesoporous in TIPOP.<sup>5</sup> The intense peaks at 7.2, 10.86, 21.86, 25.96, 28.36, 30.85 and 35.9° were observed in the XRD pattern. Nevertheless, due to the absorption of water from the atmosphere TIPOP have a relatively poor crystallinity.<sup>5</sup> In the XRD pattern of TMIPOP, decoration of TIPOP with FeCl<sub>3</sub> leads to a change in the pattern of peaks that revealed the successful formation of the desired catalyst.

EDX analysis was applied to confirm the elemental composition of TMIPOP; the signals of C, N, Cl and Fe were depicted in

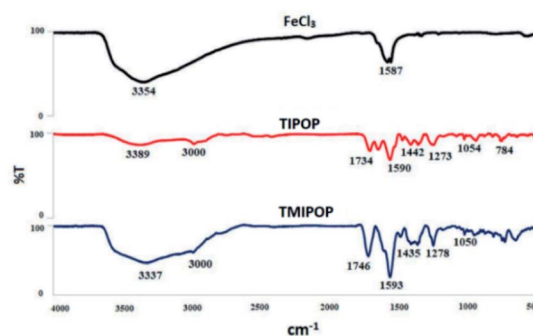


Fig. 1 FT-IR spectra of FeCl<sub>3</sub>, TIPOP, TMIPOP.

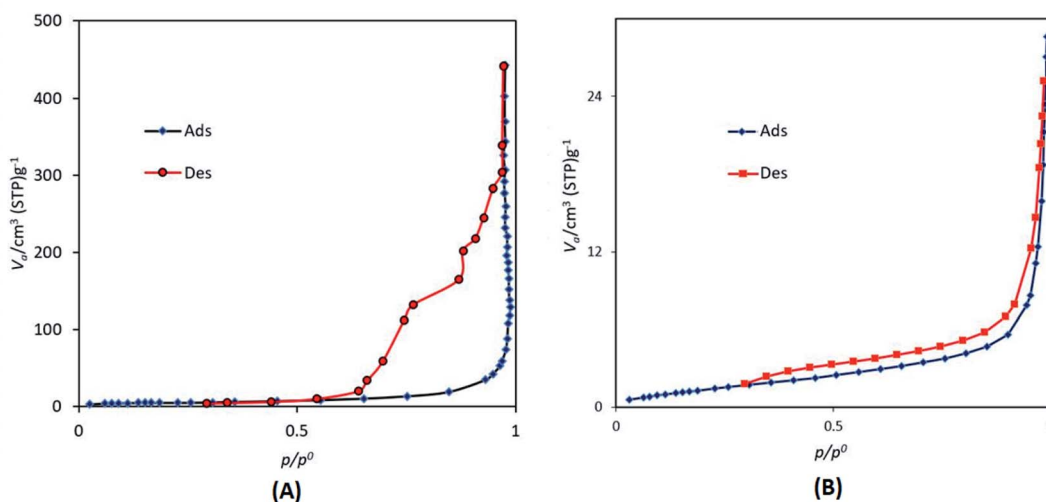


Fig. 2 (A):  $N_2$  adsorption-desorption isotherm of TIPOP, (B):  $N_2$  adsorption-desorption isotherm of TMIPOP.

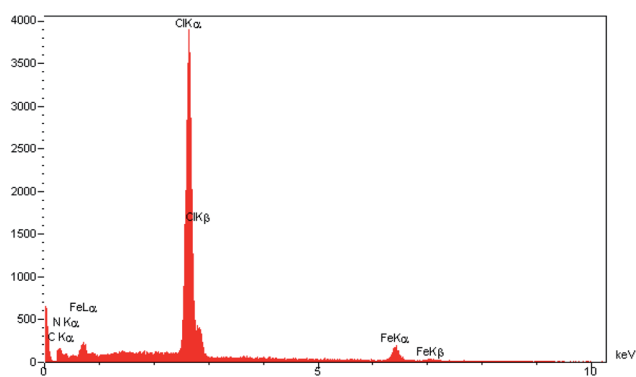


Fig. 3 EDX analysis of TMIPOP.

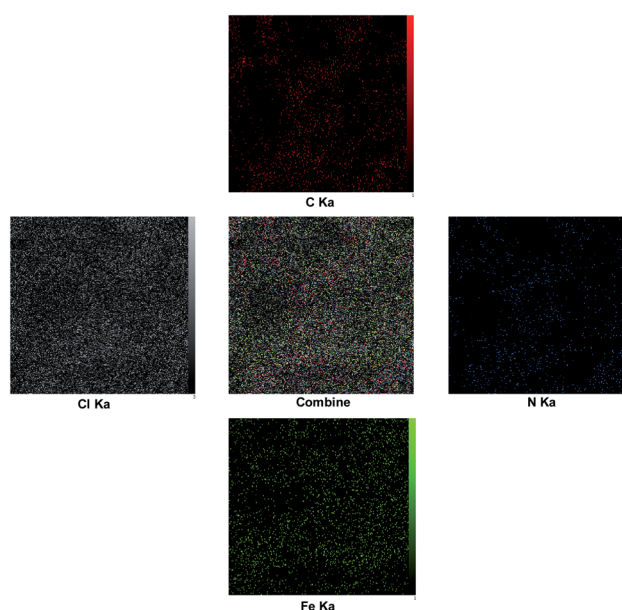


Fig. 4 Elemental mapping analysis of TMIPOP.

Moreover, elemental mapping analysis shows the uniform distribution of all elements (Fig. 4).

The thermal stability of TMIPOP was tested with TG/DTG analysis (see ESI†). The sample was heated at the rate of  $10\text{ }^{\circ}\text{C min}^{-1}$  under a nitrogen atmosphere from ambient temperature to  $600\text{ }^{\circ}\text{C}$ . A little weight loss in the range of about  $80\text{--}130\text{ }^{\circ}\text{C}$  is related to adsorbed water and trapped solvents in the pores. The two-loss weight indicates that the catalyst has good thermal stability up to  $200\text{ }^{\circ}\text{C}$ .

The morphology of TMIPOP was investigated by scanning electron microscopy (SEM) and transmission electron microscopy (TEM) analysis. SEM analysis revealed that the prepared sample has both regular and irregular surface morphology (Fig. 5). Interestingly, consistent with the prediction from the structure of applied starting materials, the obtained TEM images reveal unique hexagonal morphology for the TMIPOP (Fig. 6).

After synthesis and characterization of TMIPOP, we applied it as a catalyst for the synthesis of hybrid pyridine derivatives bearing indole, triazole and sulfonamide sections. Herein, we synthesized *N*-(4-(4-acetyl-5-methyl-1*H*-1,2,3-triazol-1-yl)phenyl)-4-methylbenzenesulfonamide (**ke3**) for the first time (Scheme 3). Then, **ke3**, 4-chlorobenzaldehyde, 3-(1*H*-indol-3-yl)-3-

oxopropanenitrile and ammonium acetate were selected for multicomponent synthesis of hybrid pyridine derivatives as a model reaction. To gain the optimized conditions, the effect of different parameters such as solvent, temperature and amount of catalyst were evaluated. The reaction was performed in the presence of different protic and aprotic solvents. Polar solvents inactivated the active sites of the catalyst. Specifically, the catalyst was dissolved in water and in aprotic solvents relatively better results were observed for the synthesis of pyridine derivatives. But, solvent-free conditions were selected as the best conditions. In the optimization of temperature,  $110\text{ }^{\circ}\text{C}$  was emerged as the best temperature to supply the activation energy of the reaction. In the optimization of the amount of catalyst, three different amounts of catalyst were tested which obtained results indicate that 20 mg of





Fig. 5 SEM images of TMIPOP.

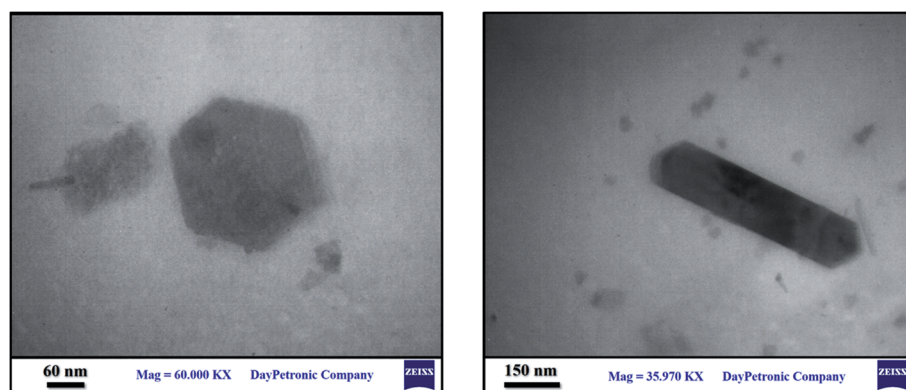


Fig. 6 TEM images of TMIPOP.

catalyst is the best choice. In the absence of a catalyst, not enough progress was made in the reaction (Table 1).

In another investigation, to prove the capabilities of the catalyst, the model reaction was performed with TMIPOP and its related intermediates and several known catalysts. According to results (Table 2), TMIPOP has a relatively higher capability than other catalysts.

Under the preferred conditions (20 mg of TMIPOP was used as the catalyst under the solvent-free condition at 110 °C) the substrate scope for the general validity of hybrid pyridines was studied. As a sequence, a variety of aromatic aldehydes with electron-poor or electron-rich aryl groups were used for the synthesis of pyridine derivatives. In this system, the role of electron-poor or electron-rich aryl groups has no effect on the progress of reactions (Table 3).

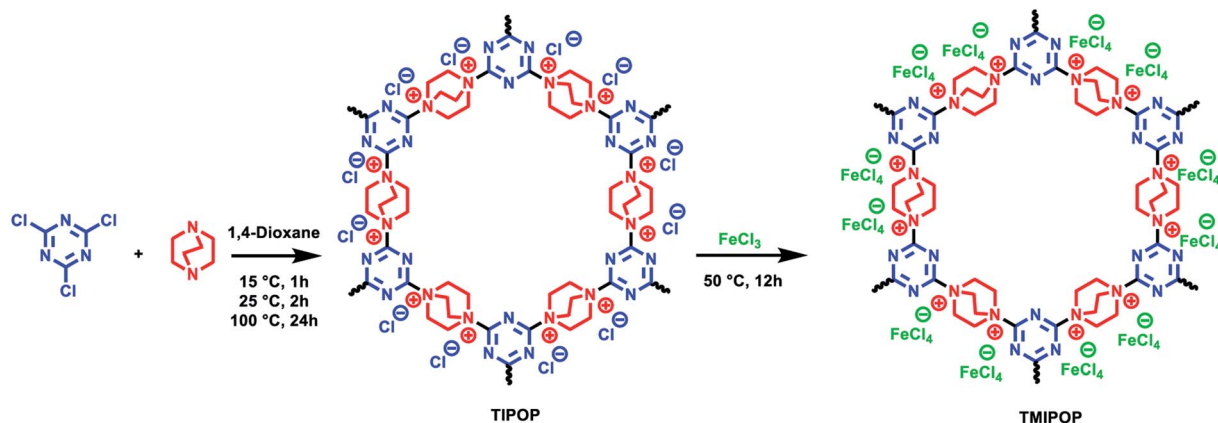
In organic synthesis, recycling and reusing the catalyst is a critical issue. In this regard, the recycling and reusing test of TMIPOP was investigated upon the synthesis of molecule **1a** as a model reaction under optimal reaction conditions. After running and completing each of the reactions, the mixture was dissolved in 10 mL ethanol at 25 °C. In this condition, unreacted starting materials, intermediates and product are soluble but the catalyst is insoluble. After centrifuging the mixture of reaction, the catalyst was separated and washed three times with cold ethanol. This process was performed five times and the efficiency of the catalyst has not significantly dropped (Scheme 4).

Based on a detailed study, a plausible mechanism for the synthesis of target molecule **1a** (Scheme 5) is presented. Firstly, the carbonyl group of **ke3** was activated with a catalyst and reacted with ammonia (arising from thermal dissociation of ammonium acetate). After that *via* a tautomerization process, the intermediate (**A**) was formed. In another reaction, the carbonyl group of benzaldehyde was activated with catalyst and through the reaction with 3-(1*H*-indol-3-yl)-3-oxopropanenitrile leads to the formation of Knoevenagel intermediate (**B**). Then, due to the reaction of intermediates (**A**) and (**B**) and followed by a tautomerization process, the intermediate (**C**) was produced. In the next step, the intermediate (**D**) was formed *via* an intramolecular nucleophilic attack. Then, the key intermediate (**E**) was synthesized through a dehydration process. In the next step, the NH group of dihydropyridine was activated with the anionic part of the catalyst which leads to separation and releasing of hydrogen. Finally, the target product was synthesized *via* a cooperative vinylogous anomeric-based oxidation.<sup>57–59</sup>

## Experimental section

### General experimental procedure for the synthesis of TMIPOP

At the first, TIPOP was synthesized similar to the reported procedure.<sup>5</sup> The TIPOP was synthesized by the reaction of diazabicyclo[2.2.2]octane (DABCO) and cyanuric chloride. DABCO (1.68 g, 15 mmol) was dissolved in 1,4-dioxane (200 mL) and

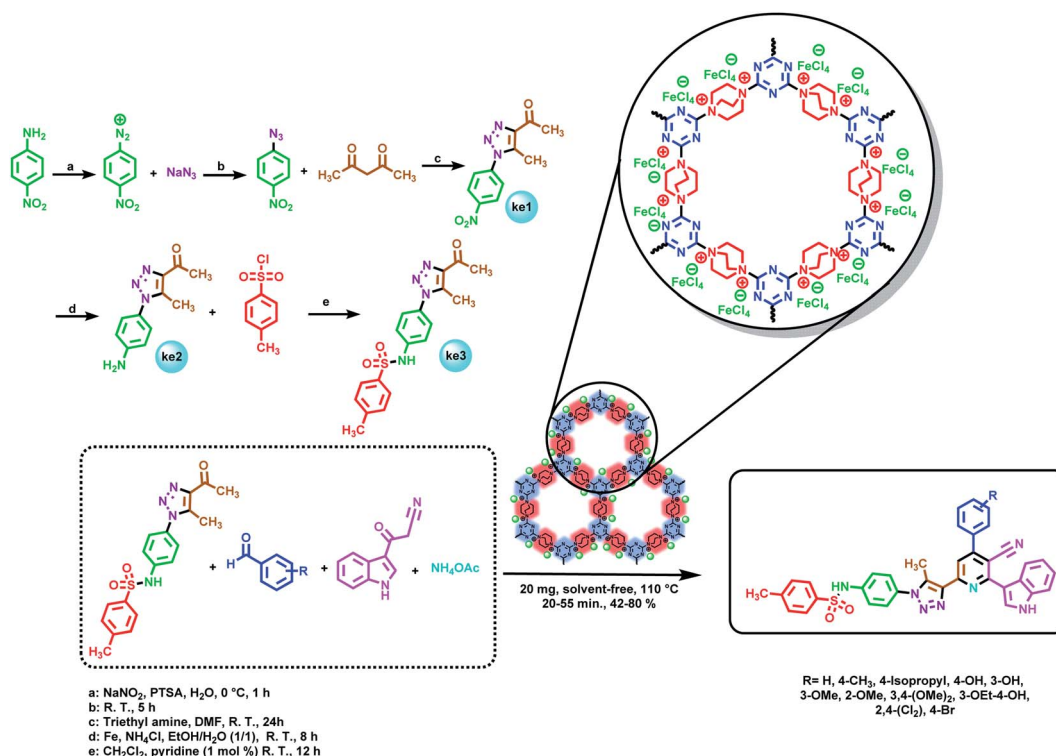


Scheme 2 General procedure for the synthesis of TMIPOP.

cyanuric chloride (1.84 g, 10 mmol) was dissolved in 1,4-dioxane (100 mL) and was added drop-wise to the DABCO solution and stirred for 1 h at 15 °C. After that, the mixture was stirred for 2 h at room temperature. In the next step, the solution was vigorously stirred at 100 °C for 24 h. After the completion of the reaction, the white precipitate was filtered and washed with THF, 1,4-dioxane and acetone three times. Then, the product was dried at 120 °C for 12 h. Finally, FeCl<sub>3</sub> (2.43 g, 15 mmol) was added to the 1.76 g TIPOP and heated at 60 °C for 12 h under N<sub>2</sub> atmosphere. Therefore, the yellow product (TMIPOP) was formed.

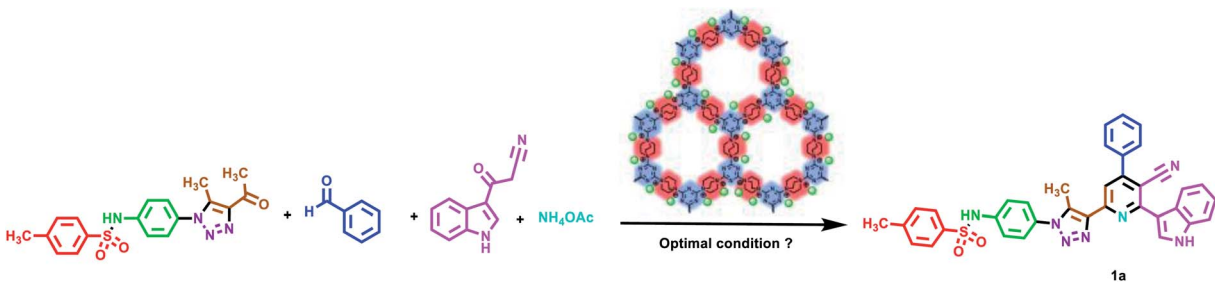
### General experimental procedure for the synthesis of ke3

Initially, 1-azido-4-nitrobenzene was prepared according to the general reported procedure.<sup>64</sup> After that, 1-azido-4-nitrobenzene (1.64 g, 10 mmol) and acetyl acetone (1.5 g, 15 mmol) were added to the 50 mL of DMF and 2 mL of triethyl amine as catalyst was added drop-wise to this solution and stirred at 25 °C for 24 h. After completing the reaction, 200 mL of distilled water was added to obtain a bulky precipitate which was filtered and washed with distilled water to obtain a pure product of **ke1** with 92% yield. In the second step, NH<sub>4</sub>Cl (8.92 g, 168 mmol) and iron powder (9.4 g, 168 mmol) were added to the solution of



Scheme 3 General experimental procedure for the synthesis of hybrid pyridines using TMIPOP as catalyst.



Table 1 Optimizing of the reaction conditions for the synthesis of **1a**<sup>a</sup>


Entry	Solvent	Temperature (°C)	Catalyst loading (mg)	Time (min.)	Yield <sup>b</sup> (%)
1	—	120	20	20	80
2 <sup>c</sup>	—	110	20	20	80
3	—	110	30	20	78
4	—	110	10	20	67
5	—	110	—	20	Trace
6	—	110	—	120	45
7	—	100	20	30	50
8	—	90	20	60	40
9	—	80	20	60	Trace
11	H <sub>2</sub> O	Reflux	20	240	—
12	EtOH	Reflux	20	240	—
13	<i>n</i> -Hexane	Reflux	20	240	Trace
14	EtOAc	Reflux	20	240	35
15	CH <sub>2</sub> Cl <sub>2</sub>	Reflux	20	240	20
16	THF	Reflux	20	240	45

<sup>a</sup> Reaction conditions: benzaldehyde (1 mmol, 0.106 g), **ke3** (1 mmol, 0.370 g), 3-(1*H*-indol-3-yl)-3-oxopropanenitrile (1 mmol, 0.184 g) and ammonium acetate (1.5 mmol, 0.115 g). <sup>b</sup> Related to isolated yields. <sup>c</sup> Optimal data.

Table 2 Investigation of catalytic behaviour of TMIPOP and its relative intermediates and other known catalysts upon the synthesis of **1a**<sup>a</sup>

Entry	Catalyst	Load of catalyst	Yield (%)
1	TIPOP	20 mg	62
2	FeCl <sub>3</sub>	20 mol%	35
3	TMIPOP	20 mg	80
4	HCl	20 mol%	Trace
5	AlCl <sub>3</sub>	20 mol%	25
6	H <sub>2</sub> SO <sub>4</sub>	20 mol%	45
7	Trityl chloride	20 mol%	30
8	Trityl bromide	20 mol%	42
9	Silica sulfuric acid (SSA) <sup>63</sup>	20 mg	75
10	NH <sub>2</sub> SO <sub>3</sub> H	20 mol%	20
11	Fe(HSO <sub>4</sub> ) <sub>3</sub>	20 mol%	35
12	Al(HSO <sub>4</sub> ) <sub>3</sub>	20 mol%	30
13	Ca(HSO <sub>4</sub> ) <sub>2</sub>	20 mol%	25

<sup>a</sup> Reaction conditions: benzaldehyde (1 mmol, 0.106 g), **ke3** (1 mmol, 0.370 g), 3-(1*H*-indol-3-yl)-3-oxopropanenitrile (1 mmol, 0.184 g) and ammonium acetate (1.5 mmol, 0.115 g). Solvent-free, 110 °C, 45 min.

water and ethanol (140 mL, v/v = 1/1) in a 250 mL flask. The suspension was heated at 60 °C for 30 min while vigorously stirred. **ke1** (6.4 g, 26 mmol) was then added in 10 min and the reaction temperature was raised to 80 °C. After completing the reaction, the mixture was cooled to room temperature and

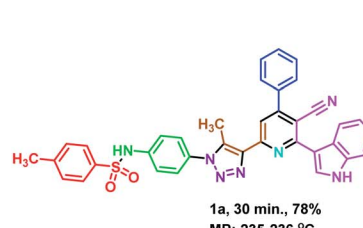
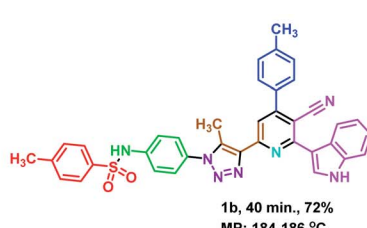
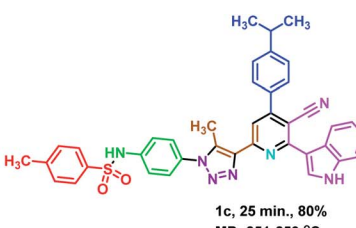
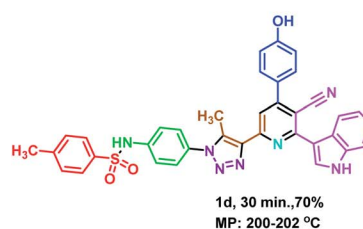
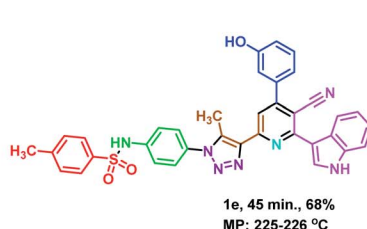
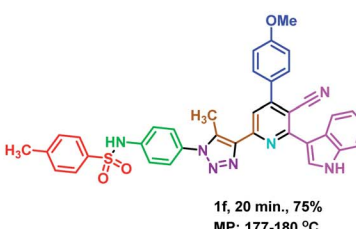
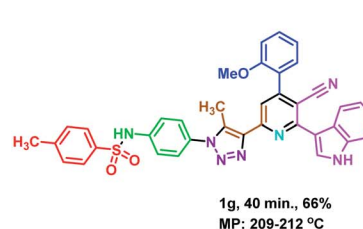
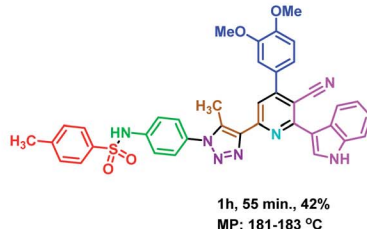
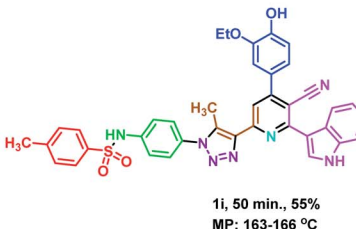
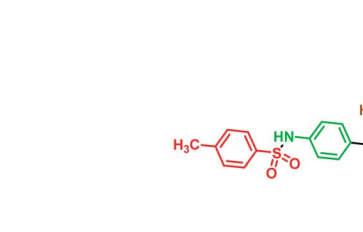
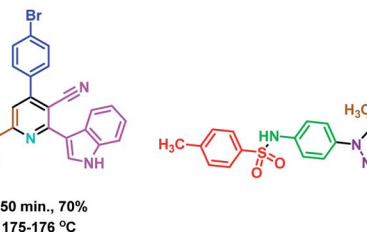
basified with NaOH. In the next step, the mixture was filtrated to removing of all iron powder. The remained solution was evaporated and extracted with EtOAc and H<sub>2</sub>O. After separation of the organic phase, the solvent was evaporated to give pure product (**ke2**) with 95% yield. In the third step, **ke2** (2.16 g, 10 mmol) and 4-methylbenzenesulfonyl chloride (2.28 g, 12 mmol) was dissolved in CH<sub>2</sub>Cl<sub>2</sub> (100 mL) and 1 mL of pyridine was added as catalyst and the mixture was stirred at 25 °C for 24 h. After completing of reaction, the solvent was removed and the remained product was washed with water and ethanol to obtain pure solid. Finally, the white product (**ke3**) dried at 80 °C (yield: 96%).

#### General procedure for the synthesis of hybrid pyridines using TMIPOP as catalyst

Aromatic aldehydes (1 mmol), **ke3** (0.370, 1 mmol), 3-(1*H*-indol-3-yl)-3-oxopropanenitrile (0.184 g, 1 mmol), ammonium acetate (1.5 mmol, 0.115 g) and TMIPOP (0.02 g) were successively added into a 10 mL round-bottomed flask under an air atmosphere and the mixture of reaction was stirred vigorously at 110 °C. The progress of the reaction was observed by thin-layer chromatography. After completing each reaction, the solid was dissolved in 10 mL ethanol at 25 °C and was centrifuged to separate the catalyst. Finally, each product was purified by TLC plate techniques with *n*-hexane/ethyl acetate as eluent.



Table 3 Synthesis of hybrid pyridine derivatives in the presence of TMIPOP as catalyst<sup>a</sup>

 <p><b>1a</b>, 30 min., 78% MP: 235–236 °C</p>	 <p><b>1b</b>, 40 min., 72% MP: 184–186 °C</p>	 <p><b>1c</b>, 25 min., 80% MP: 251–253 °C</p>
 <p><b>1d</b>, 30 min., 70% MP: 200–202 °C</p>	 <p><b>1e</b>, 45 min., 68% MP: 225–226 °C</p>	 <p><b>1f</b>, 20 min., 75% MP: 177–180 °C</p>
 <p><b>1g</b>, 40 min., 66% MP: 209–212 °C</p>	 <p><b>1h</b>, 55 min., 42% MP: 181–183 °C</p>	 <p><b>1i</b>, 50 min., 55% MP: 163–166 °C</p>
 <p><b>1m</b>, 50 min., 70% MP: 175–176 °C</p>	 <p><b>1l</b>, 30 min., 75% MP: 185–186 °C</p>	

<sup>a</sup> Reaction conditions: aldehyde (1 mmol), **ke3** (1 mmol, 0.370 g), 3-(1*H*-indol-3-yl)-3-oxopropanenitrile (1 mmol, 0.184 g) and ammonium acetate (1.5 mmol, 0.115 g), solvent-free, 110 °C, catalyst = 20 mg, reported yields are referred to isolated yields.

## Spectral data

### 1-(5-Methyl-1-(4-nitrophenyl)-1*H*-1,2,3-triazol-4-yl)ethan-1-one (**ke1**)

Mp = 132–134 °C, FT-IR (KBr,  $\nu$ ,  $\text{cm}^{-1}$ ): 2850, 1680, 1530, 1344. <sup>1</sup>H NMR (301 MHz, DMSO)  $\delta$  8.49 (dd,  $J$  = 9, 3 Hz, 2H), 7.99 (dd,  $J$  = 9, 3 Hz, 2H), 2.66 (d,  $J$  = 3 Hz, 3H), 2.61 (d,  $J$  = 3 Hz, 3H). <sup>13</sup>C NMR (76 MHz, DMSO)  $\delta$  193.7, 148.4, 143.6, 140.3, 138.7, 127.0, 125.6, 28.1, 10.3.

### 1-(1-(4-Aminophenyl)-5-methyl-1*H*-1,2,3-triazol-4-yl)ethan-1-one (**ke2**)

Mp = 170–173 °C, FT-IR (KBr,  $\nu$ ,  $\text{cm}^{-1}$ ): 3464, 3368, 3235, 1669, 1552, 1370, 1304. <sup>1</sup>H NMR (301 MHz, DMSO)  $\delta$  7.20 (d,  $J$  = 6 Hz, 2H), 6.74 (d,  $J$  = 6 Hz, 2H), 5.67 (s, 2H), 2.61 (s, 3H), 2.45 (s, 3H). <sup>13</sup>C NMR (76 MHz, DMSO)  $\delta$  193.8, 150.8, 143.0, 137.9, 126.7, 123.4, 114.0, 27.9, 10.1.

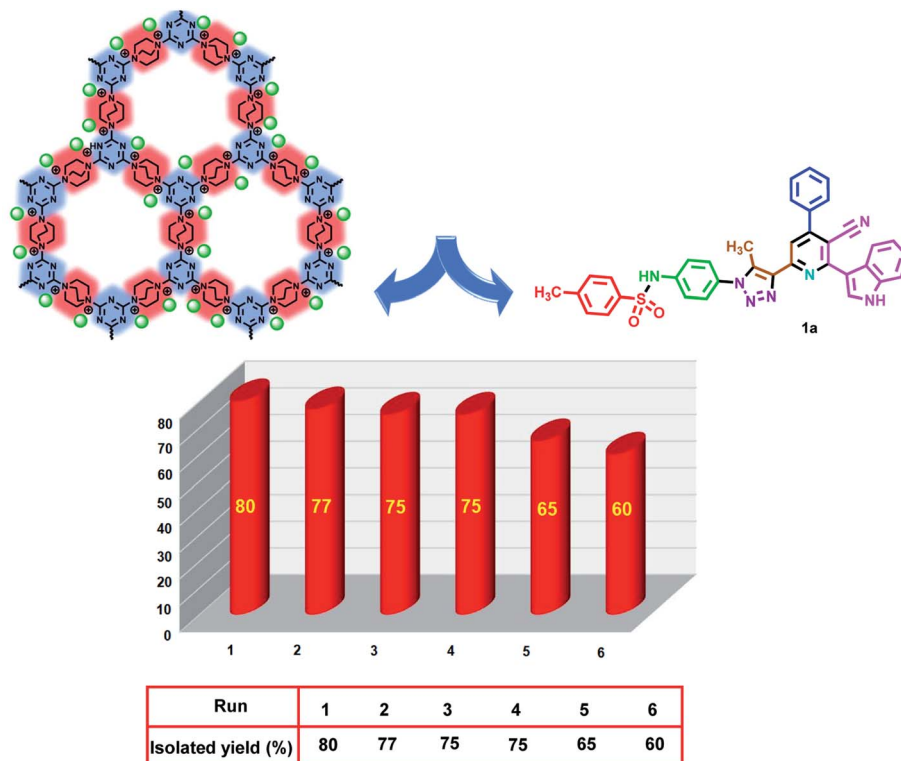
### *N*-(4-(4-Acetyl-5-methyl-1*H*-1,2,3-triazol-1-yl)phenyl)-4-methylbenzenesulfonamide (**ke3**)

Mp = 159–160 °C, FT-IR (KBr,  $\nu$ ,  $\text{cm}^{-1}$ ): 3231, 2925, 1668, 1515, 1422, 1337. <sup>1</sup>H NMR (301 MHz, DMSO)  $\delta$  10.77 (s, 1H), 7.76 (d,  $J$  = 6 Hz, 2H), 7.53 (d,  $J$  = 9 Hz, 2H), 7.41 (d,  $J$  = 9 Hz, 2H), 7.34 (d,  $J$  = 9 Hz, 2H), 2.62 (s, 3H), 2.45 (s, 3H), 2.36 (s, 3H). <sup>13</sup>C NMR (76 MHz, DMSO)  $\delta$  193.8, 144.2, 143.2, 140.0, 138.1, 136.9, 130.7, 130.4, 127.2, 126.9, 120.0, 28.0, 21.5, 10.1.

### *N*-(4-(4-(5-Cyano-6-(1*H*-indol-3-yl)-4-phenylpyridin-2-yl)-5-methyl-1*H*-1,2,3-triazol-1-yl)phenyl)-4-methylbenzenesulfonamide (**1a**)

Mp = 235–236 °C, FT-IR (KBr,  $\nu$ ,  $\text{cm}^{-1}$ ): 3405, 3228, 3060, 2926, 2213, 1588, 1515, 1340, 1164. <sup>1</sup>H NMR (301 MHz, DMSO)  $\delta$  11.89 (s, 1H), 8.31–8.23 (m, 2H), 8.08 (s, 1H), 7.83–7.81 (m, 2H), 7.74–7.64 (m, 4H), 7.56 (d,  $J$  = 6 Hz, 1H), 7.44–7.17 (m, 10H), 2.70 (s, 3H), 2.35 (s, 3H). <sup>13</sup>C NMR (76 MHz, DMSO)  $\delta$  158.2, 155.0,





Scheme 4 Recovering and reusing test of TMIPOP in the synthesis of 1a.

154.0, 143.6, 142.0, 137.9, 137.2, 136.8, 135.4, 130.3, 130.2, 130.0, 129.4, 129.2, 129.1, 127.2, 127.1, 126.8, 126.3, 122.8, 121.6, 121.0, 120.2, 119.1, 116.8, 113.4, 112.6, 102.1, 21.4, 10.9.

***N*-(4-(4-(5-Cyano-6-(1*H*-indol-3-yl)-4-(*p*-tolyl)pyridin-2-yl)-5-methyl-1*H*-1,2,3-triazol-1-yl)phenyl)-4-methylbenzenesulfonamide (1b)**

Mp = 184–186 °C, FT-IR (KBr,  $\nu$ ,  $\text{cm}^{-1}$ ): 3428, 3232, 2922, 2213, 1587, 1515, 1335, 1163.  $^1\text{H}$  NMR (301 MHz, DMSO)  $\delta$  11.88 (s, 1H), 8.29 (d,  $J$  = 3 Hz, 1H), 8.23 (d,  $J$  = 9 Hz, 1H), 8.05 (s, 1H), 7.73–7.71 (m, 4H), 7.56 (d,  $J$  = 9 Hz, 1H), 7.46–7.42 (m, 4H), 7.34 (d,  $J$  = 9 Hz, 2H), 7.27–7.15 (m, 5H), 2.69 (s, 3H), 2.45 (s, 3H), 2.35 (s, 3H).  $^{13}\text{C}$  NMR (76 MHz, DMSO)  $\delta$  158.2, 155.0, 153.9, 143.5, 142.0, 140.2, 138.0, 136.8, 135.4, 134.3, 130.2, 130.0, 129.2, 129.1, 127.2, 126.8, 126.2, 122.8, 121.6, 121.0, 120.2, 119.3, 116.7, 113.4, 112.6, 102.0, 21.4, 21.4, 10.9. MS ( $m/z$ ) = calcd for  $\text{C}_{37}\text{H}_{29}\text{N}_7\text{O}_2\text{S}$ : 635.75, found: 635.4.

***N*-(4-(4-(5-Cyano-6-(1*H*-indol-3-yl)-4-(4-isopropylphenyl)pyridin-2-yl)-5-methyl-1*H*-1,2,3-triazol-1-yl)phenyl)-4-methylbenzenesulfonamide (1c)**

Mp = 251–253 °C, FT-IR (KBr,  $\nu$ ,  $\text{cm}^{-1}$ ): 3414, 3222, 3063, 2961, 2216, 1590, 1517, 1336, 1161.  $^1\text{H}$  NMR (301 MHz, DMSO)  $\delta$  11.86 (d,  $J$  = 3 Hz, 1H), 8.30 (d,  $J$  = 3 Hz, 1H), 8.23 (d,  $J$  = 6 Hz, 1H), 8.06 (s, 1H), 7.75 (dd,  $J$  = 9, 6 Hz, 4H), 7.57–7.48 (m, 4H), 7.38–7.15 (m, 8H), 3.04 (s,  $J$  = 6 Hz, 1H), 2.69 (s, 3H), 2.36 (s, 3H), 1.31 (d,  $J$  = 6 Hz, 6H).  $^{13}\text{C}$  NMR (76 MHz, DMSO)  $\delta$  158.2, 154.8, 153.9, 150.9, 143.9, 142.0, 140.7, 137.5, 136.8, 135.4, 134.6,

130.8, 130.3, 129.2, 129.2, 127.3, 127.2, 126.9, 126.3, 122.8, 121.6, 121.0, 120.2, 119.3, 116.8, 113.4, 112.5, 101.9, 33.8, 24.2, 21.4, 10.9. MS ( $m/z$ ) = calcd for  $\text{C}_{39}\text{H}_{33}\text{N}_7\text{O}_2\text{S}$ : 663.8, found: 663.

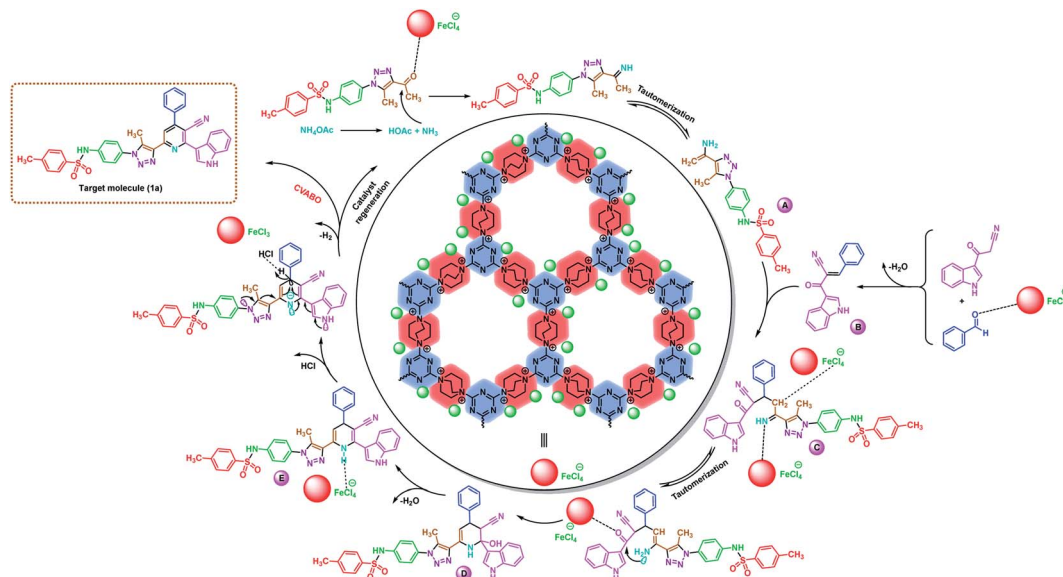
***N*-(4-(4-(5-Cyano-4-(4-hydroxyphenyl)-6-(1*H*-indol-3-yl)pyridin-2-yl)-5-methyl-1*H*-1,2,3-triazol-1-yl)phenyl)-4-methylbenzenesulfonamide (1d)**

Mp = 200–202 °C, FT-IR (KBr,  $\nu$ ,  $\text{cm}^{-1}$ ): 3371, 3261, 2923, 2216, 1705, 1594, 1517, 1339, 1160.  $^1\text{H}$  NMR (301 MHz, DMSO)  $\delta$  11.86 (s, 1H), 8.28 (d,  $J$  = 3 Hz, 1H), 8.22 (d,  $J$  = 9 Hz, 1H), 8.03 (s, 1H), 7.73 (s, 1H), 7.70 (d,  $J$  = 3 Hz, 2H), 7.66 (s, 1H), 7.55 (d,  $J$  = 9 Hz, 1H), 7.40 (d,  $J$  = 9 Hz, 2H), 7.32 (d,  $J$  = 9 Hz, 2H), 7.27–7.24 (m, 1H), 7.20 (dd,  $J$  = 6, 1.4 Hz, 1H), 7.17–7.15 (m, 3H), 7.02 (d,  $J$  = 9 Hz, 2H), 6.71 (d,  $J$  = 6 Hz, 1H), 2.68 (s, 3H), 2.34 (s, 3H).  $^{13}\text{C}$  NMR (76 MHz, DMSO)  $\delta$  159.7, 158.2, 156.9, 154.6, 153.9, 141.9, 136.8, 135.2, 130.8, 129.8, 129.4, 127.3, 127.0, 126.4, 122.7, 121.4, 120.3, 116.4, 116.2, 115.6, 113.3, 112.5, 105.5, 102.0, 21.4, 11.0.

***N*-(4-(4-(5-Cyano-4-(3-hydroxyphenyl)-6-(1*H*-indol-3-yl)pyridin-2-yl)-5-methyl-1*H*-1,2,3-triazol-1-yl)phenyl)-4-methylbenzenesulfonamide (1e)**

Mp = 225–226 °C, FT-IR (KBr,  $\nu$ ,  $\text{cm}^{-1}$ ): 3376, 3205, 2968, 2216, 1585, 1518, 1340, 1159.  $^1\text{H}$  NMR (301 MHz, DMSO)  $\delta$  11.87 (s, 1H), 9.94 (s, 1H), 8.31–8.25 (m, 2H), 8.05 (s, 1H), 7.78 (d,  $J$  = 9 Hz, 2H), 7.59 (d,  $J$  = 9 Hz, 3H), 7.46–7.19 (m, 10H), 7.03 (d,  $J$  = 9 Hz, 1H), 2.71 (s, 3H), 2.37 (s, 3H).  $^{13}\text{C}$  NMR (76 MHz, DMSO)  $\delta$  158.2, 158.1, 155.0, 153.9, 143.9, 142.0, 140.4, 138.4, 137.4, 136.8, 135.4, 131.0, 130.5, 130.3, 129.2, 127.2, 126.9, 126.3,





Scheme 5 A plausible mechanism for the synthesis of **1a** in the presence of TMIPOP as catalyst.

122.8, 121.6, 121.0, 120.2, 119.8, 119.1, 117.3, 116.7, 115.8, 113.4, 112.6, 102.06, 21.5, 10.9.

***N*-(4-(4-(5-Cyano-6-(1*H*-indol-3-yl)-4-(4-methoxyphenyl)pyridin-2-yl)-5-methyl-1*H*-1,2,3-triazol-1-yl)phenyl)-4-methylbenzenesulfonamide (**1f**)**

Mp = 177–180 °C, FT-IR (KBr,  $\nu$ ,  $\text{cm}^{-1}$ ): 3345, 3057, 2216, 1607, 1512, 1251, 1161.  $^1\text{H}$  NMR (301 MHz, DMSO)  $\delta$  11.87 (s, 1H), 8.30 (s, 1H), 8.23 (d,  $J$  = 6 Hz, 1H), 8.05 (s, 1H), 7.80–7.74 (m, 4H), 7.57–7.52 (m, 3H), 7.39 (d,  $J$  = 9 Hz, 2H), 7.31–7.18 (m, 7H), 3.89 (s, 3H), 2.69 (s, 3H), 2.36 (s, 3H).  $^{13}\text{C}$  NMR (76 MHz, DMSO)  $\delta$  161.1, 158.2, 154.5, 153.8, 143.9, 142.1, 140.4, 137.4, 136.8, 135.3, 131.0, 130.7, 130.3, 129.2, 129.1, 127.2, 126.9, 126.3, 122.8, 121.6, 121.0, 120.2, 119.4, 116.6, 114.8, 114.1, 113.5, 112.5, 101.9, 55.8, 21.4, 10.9. MS ( $m/z$ ) = calcd for  $\text{C}_{37}\text{H}_{29}\text{N}_7\text{O}_3\text{S}$ : 651.75, found: 651.4.

***N*-(4-(4-(5-Cyano-6-(1*H*-indol-3-yl)-4-(2-methoxyphenyl)pyridin-2-yl)-5-methyl-1*H*-1,2,3-triazol-1-yl)phenyl)-4-methylbenzenesulfonamide (**1g**)**

Mp = 209–212 °C, FT-IR (KBr,  $\nu$ ,  $\text{cm}^{-1}$ ): 3330, 3067, 2961, 2216, 1601, 1588, 1519, 1440, 1159.  $^1\text{H}$  NMR (301 MHz, DMSO)  $\delta$  11.84 (d,  $J$  = 3 Hz, 1H), 10.77 (s, 1H), 8.26–8.23 (m, 2H), 7.99 (s, 1H), 7.76 (d,  $J$  = 8.3 Hz, 2H), 7.60–7.49 (m, 5H), 7.40 (d,  $J$  = 9 Hz, 2H), 7.33 (d,  $J$  = 9 Hz, 2H), 7.30–7.25 (m, 2H), 7.23–7.15 (m, 2H), 3.88 (s, 3H), 2.70 (s, 3H), 2.37 (s, 3H).  $^{13}\text{C}$  NMR (76 MHz, DMSO)  $\delta$  157.3, 156.6, 153.8, 152.8, 143.9, 142.1, 140.5, 137.4, 136.9, 135.3, 131.9, 131.0, 130.7, 130.3, 128.9, 127.2, 126.9, 126.2, 126.0, 122.8, 121.6, 121.3, 121.0, 120.2, 118.8, 117.9, 113.3, 112.6, 112.4, 104.1, 56.1, 21.5, 10.9.

***N*-(4-(4-(5-Cyano-4-(3,4-dimethoxyphenyl)-6-(1*H*-indol-3-yl)pyridin-2-yl)-5-methyl-1*H*-1,2,3-triazol-1-yl)phenyl)-4-methylbenzenesulfonamide (**1h**)**

Mp = 181–183 °C, FT-IR (KBr,  $\nu$ ,  $\text{cm}^{-1}$ ): 3390, 3337, 3063, 2922, 2216, 1616, 1516, 1260, 1160.  $^1\text{H}$  NMR (301 MHz, DMSO)  $\delta$  11.87

(d,  $J$  = 3 Hz, 1H), 8.31 (d,  $J$  = 2.7 Hz, 1H), 8.24 (d,  $J$  = 9 Hz, 1H), 8.09 (s, 1H), 7.75 (d,  $J$  = 9 Hz, 2H), 7.57–7.43 (m, 4H), 7.37 (d,  $J$  = 9 Hz, 2H), 7.30–7.15 (m, 6H), 6.88 (s, 1H), 3.90–3.89 (m, 6H), 2.69 (s, 3H), 2.36 (s, 3H).  $^{13}\text{C}$  NMR (76 MHz, DMSO)  $\delta$  158.2, 154.8, 153.8, 150.7, 149.2, 143.3, 142.1, 138.5, 136.8, 135.3, 130.1, 129.4, 129.2, 127.1, 126.7, 126.3, 122.8, 122.1, 121.8, 121.6, 121.0, 120.2, 119.5, 116.7, 113.5, 112.86, 112.5, 112.3, 111.8, 102.1, 56.2, 56.1, 21.4, 10.9.

***N*-(4-(4-(5-Cyano-4-(3-ethoxy-4-hydroxyphenyl)-6-(1*H*-indol-3-yl)pyridin-2-yl)-5-methyl-1*H*-1,2,3-triazol-1-yl)phenyl)-4-methylbenzenesulfonamide (**1i**)**

Mp = 163–166 °C, FT-IR (KBr,  $\nu$ ,  $\text{cm}^{-1}$ ): 3399, 3251, 2926, 2212, 1587, 1513, 1434, 1159.  $^1\text{H}$  NMR (301 MHz, DMSO)  $\delta$  11.85 (d,  $J$  = 3 Hz, 1H), 9.60 (s, 1H), 8.30 (d,  $J$  = 3 Hz, 1H), 8.22 (d,  $J$  = 9 Hz, 1H), 8.06 (s, 1H), 7.75 (d,  $J$  = 9 Hz, 2H), 7.56–7.50 (m, 3H), 7.42–7.36 (m, 3H), 7.31–7.14 (m, 7H), 7.03 (d,  $J$  = 9 Hz, 1H), 4.18 (q,  $J$  = 6 Hz, 2H), 2.69 (s, 3H), 2.36 (s, 3H), 1.41 (t,  $J$  = 6 Hz, 3H).  $^{13}\text{C}$  NMR (76 MHz, DMSO)  $\delta$  158.3, 154.7, 153.7, 149.2, 147.2, 143.7, 142.0, 136.8, 135.2, 130.1, 129.1, 127.7, 127.1, 126.8, 126.5, 123.6, 122.7, 122.4, 121.2, 120.9, 120.2, 119.4, 116.1, 114.7, 112.7, 102.0, 64.6, 21.4, 15.2, 10.9.

***N*-(4-(4-(4-(4-Bromophenyl)-5-cyano-6-(1*H*-indol-3-yl)pyridin-2-yl)-5-methyl-1*H*-1,2,3-triazol-1-yl)phenyl)-4-methylbenzenesulfonamide (**1j**)**

Mp = 175–176 °C, FT-IR (KBr,  $\nu$ ,  $\text{cm}^{-1}$ ): 3383, 3241, 2922, 2216, 1593, 1514, 1333, 1158.  $^1\text{H}$  NMR (301 MHz, DMSO)  $\delta$  11.88 (s, 1H), 8.30 (d,  $J$  = 3 Hz, 1H), 8.24 (d,  $J$  = 9 Hz, 1H), 8.06 (s, 1H), 7.86 (d,  $J$  = 9 Hz, 2H), 7.79–7.74 (m, 4H), 7.58–7.54 (m, 3H), 7.40 (d,  $J$  = 6 Hz, 2H), 7.33 (d,  $J$  = 9 Hz, 2H), 7.27–7.15 (m, 3H), 2.70 (s, 3H), 2.36 (s, 3H).  $^{13}\text{C}$  NMR (76 MHz, DMSO)  $\delta$  158.2, 154.1, 153.8, 144.0, 142.0, 137.0, 136.8, 136.3, 135.5, 132.4, 131.4,



131.2, 130.3, 129.3, 127.2, 126.9, 124.1, 122.9, 121.6, 121.0, 120.2, 119.0, 116.7, 113.4, 112.6, 102.0, 21.4, 10.9.

**N-(4-(4-(5-Cyano-4-(2,4-dichlorophenyl)-6-(1H-indol-3-yl)pyridin-2-yl)-5-methyl-1H-1,2,3-triazol-1-yl)phenyl)-4-methylbenzenesulfonamide (1k)**

Mp = 185–186 °C, FT-IR (KBr,  $\nu$ ,  $\text{cm}^{-1}$ ): 3406, 3261, 2968, 2216, 1596, 1513, 1430, 1162.  $^1\text{H}$  NMR (301 MHz, DMSO)  $\delta$  11.91 (s, 1H), 8.29–8.26 (m, 2H), 8.01 (s, 1H), 7.95 (d,  $J$  = 2 Hz, 1H), 7.76–7.68 (m 4H), 7.57–7.52 (m, 3H), 7.38 (d,  $J$  = 6 Hz, 2H), 7.31–7.17 (m, 5H), 2.71 (s, 3H), 2.36 (s, 3H).  $^{13}\text{C}$  NMR (76 MHz, DMSO)  $\delta$  157.6, 154.2, 151.9, 143.5, 141.9, 141.5, 138.0, 136.9, 135.7, 135.1, 133.1, 132.7, 130.3, 130.2, 129.9, 129.1, 128.5, 127.2, 126.8, 126.1, 123.0, 121.7, 121.1, 120.2, 118.1, 117.4, 113.1, 112.7, 103.2, 21.4, 11.0. MS ( $m/z$ ) = calcd for  $\text{C}_{36}\text{H}_{25}\text{Cl}_2\text{N}_7\text{O}_2\text{S}$ : 690.6, found: 689.3.

## Conclusion

In conclusion, we introduced TMIPOP as a novel series of IPOP. The magnetic susceptibility of catalyst was investigated with VSM analysis and showed that TMIPOP has paramagnetic properties. According to the observed results of TEM analysis, TMIPOP has a hexagonal structure. Then, catalytic application of TMIPOP was studied in the synthesis of new series of pyridine hybrids with triazole, sulphonamide and indole sections that were reported for the first time. According to results, TMIPOP as a green and efficient catalyst has excellent potential in multi-component reactions. This system can be converted to a drastic methodology in many areas of catalytic reactions.

## Conflicts of interest

There are no conflicts to declare.

## Acknowledgements

We thank the Bu-Ali Sina University and Iran National Science Foundation [(INSF), Grant Number: 98001912] for financial support to our research group.

## References

- 1 J. Wu, F. Xu, S. Li, P. Ma, X. Zhang, Q. Liu, R. Fu and D. Wu, *J. Adv. Mater.*, 2019, **31**, 1802922.
- 2 Y. Jin, Y. Hu and W. Zhang, *Nat. Rev. Chem.*, 2017, **1**, 1.
- 3 D. Wu, F. Xu, B. Sun, R. Fu, H. He and K. Matyjaszewski, *Chem. Rev.*, 2012, **112**, 3959.
- 4 M. Torabi, *Iran. J. Catal.*, 2021, **11**, 417.
- 5 J. Byun, H. A. Patel, D. Thirion and C. T. Yavuz, *Polymer*, 2017, **126**, 308.
- 6 Y. Tian and G. Zhu, *Chem. Rev.*, 2020, **120**, 8934.
- 7 Y. B. Zhou and Z. P. Zhan, *Chem.-Asian J.*, 2018, **13**, 9.
- 8 P. Ju, S. Wu, Q. Su, X. Li, Z. Liu, G. Li and Q. Wu, *J. Mater. Chem. A*, 2019, **7**, 2660.
- 9 C. Yadav, V. K. Maka, S. Payra and J. N. Moorthy, *J. Catal.*, 2020, **384**, 61.
- 10 D. Xu, J. Guo and F. Yan, *Prog. Polym. Sci.*, 2018, **79**, 121.
- 11 Z. W. Liu and B. H. Han, *Curr. Opin. Green Sustain. Chem.*, 2019, **16**, 20.
- 12 J. K. Sun, M. Antonietti and J. Yuan, *Chem. Soc. Rev.*, 2016, **45**, 6627.
- 13 A. S. Aricò, P. Bruce, B. Scrosati, J. M. Tarascon and W. van Schalkwijk, *Nat. Mater.*, 2015, **4**, 366.
- 14 S. Kramer, N. R. Bennedsen and S. Kegnæs, *ACS Catal.*, 2018, **8**, 6961.
- 15 S. Jayakumar, H. Li, J. Chen and Q. Yang, *ACS Appl. Mater. Interfaces*, 2018, **10**, 2546.
- 16 S. Hayashi and H. Hamaguchi, *Chem. Lett.*, 2004, **33**, 1590.
- 17 J. Lunagariya, A. Dhar and R. L. Vekariya, *RSC Adv.*, 2017, **7**, 5412.
- 18 (a) M. Torabi, M. Yarie, M. A. Zolfigol and S. Azizian, *Res. Chem. Intermed.*, 2020, **46**, 891; (b) M. R. Anizadeh, M. A. Zolfigol, M. Yarie, M. Torabi and S. Azizian, *Res. Chem. Intermed.*, 2020, **46**, 3945.
- 19 L. Qi, R. Li, X. Yao, Q. Zhen, P. Ye, Y. Shao and J. Chen, *J. Org. Chem.*, 2019, **85**, 1097.
- 20 C. Allais, J. M. Grassot, J. Rodriguez and T. Constantieux, *Chem. Rev.*, 2014, **114**, 10829.
- 21 J. A. Bull, J. J. Mousseau, G. Pelletier and A. B. Charette, *Chem. Rev.*, 2012, **112**, 2642.
- 22 C. Römel, T. Weyhermüller and K. Wieghardt, *Coord. Chem. Rev.*, 2019, **380**, 287.
- 23 Z. Chen, M. H. Y. Chan and V. W. W. Yam, *J. Am. Chem. Soc.*, 2020, **142**, 16471.
- 24 L. Goswami, S. Gogoi, J. Gogoi, R. K. Boruah, R. C. Boruah and P. Gogoi, *ACS Comb. Sci.*, 2016, **18**, 253.
- 25 M. Baumann and I. R. Baxendale, *Beilstein J. Org. Chem.*, 2013, **9**, 2265.
- 26 M. Horiuchi, C. Murakami, N. Fukamiya, D. Yu, T. H. Chen, K. F. Bastow, D. C. Zhang, Y. Takaishi, Y. Imakura, K. H. Lee and A. C. Tripfordines, *J. Nat. Prod.*, 2006, **69**, 1271.
- 27 S. M. Gomha and K. M. Dawood, *J. Heterocycl. Chem.*, 2017, **54**, 1943.
- 28 X. X. Du, Q. X. Zi, Y. M. Wu, Y. Jin, J. Lin and S. J. Yan, *Green Chem.*, 2019, **21**, 1505.
- 29 P. L. Ferrarini, C. Mori, M. Badawneh, V. Calderone, R. Greco, C. Manera, A. Martinelli, P. Nieri and G. Saccomanni, *Eur. J. Med. Chem.*, 2000, **35**, 815.
- 30 M. M. Naik, M. N. Deshpande, R. Borges, B. S. Biradar and S. G. Shingade, *J. Drug Delivery Ther.*, 2017, **7**, 202.
- 31 Y. Sajja, S. Vanguru, H. R. Vulupala, R. Bantu, P. Yogeswari, D. Sriram and L. Nagarapu, *Bioorg. Med. Chem. Lett.*, 2017, **27**, 5119.
- 32 M. F. Ahmed and E. Y. Santali, *Bioorg. Chem.*, 2021, **111**, 104842.
- 33 H. Konishi, H. Tanaka and K. Manabe, *Org. Lett.*, 2017, **19**, 1578.
- 34 D. A. Smith and R. M. Jones, *Curr. Opin. Drug Discovery Dev.*, 2008, **11**, 72.
- 35 V. Ramdas, R. Talwar, V. Kanoje, R. M. Loria, M. Banerjee, P. Patil, A. A. Joshi, L. Datrange, A. K. Das, D. S. Walke, V. Kalthapure, T. Khan, G. Gote, U. Dhayagude, S. Deshpande, J. Shaikh, G. Chaure, R. R. Pal, S. Parkale,



- S. Suravase, S. Bhoskar, R. V. Gupta, A. Kalia, R. Yeshodharan, M. Azhar, J. Daler, V. Mali, G. Sharma, A. Kishore, R. Vyawahare, G. Agarwal, H. Pareek, S. Budhe, A. Nayak, D. Warude, P. Kumar Gupta, P. Joshi, S. Joshi, S. Darekar, D. Pandey, A. Wagh, P. B. Nigade, M. Mehta, V. Patil, D. Modi, S. Pawar, M. Verma, M. Singh, S. Das, J. Gundu, K. Nemmani, M. G. Bock, S. Sharma, D. Bakhle, R. K. Kamboj and V. P. Palte, *J. Med. Chem.*, 2020, **63**, 6107.
- 36 J. J. Petkowski, W. Bains and S. Seager, Natural products containing a nitrogen-sulfur bond, *J. Nat. Prod.*, 2018, **81**, 423.
- 37 T. Q. Davies, M. J. Tilby, D. Skolc, A. Hall and M. C. Willis, *Org. Lett.*, 2020, **22**, 9495.
- 38 Y. Liu, Q. Pan, X. Hu, Y. Guo, Q. Y. Chen and C. Liu, *Org. Lett.*, 2021, **23**, 3975.
- 39 S. P. Blum, T. Karakaya, D. Schollmeyer, A. Klapars and S. R. Waldvogel, *Angew. Chem., Int. Ed.*, 2021, **60**, 5056.
- 40 S. Caddick, J. D. Wilden and D. B. Judd, *J. Am. Chem. Soc.*, 2004, **126**, 1024.
- 41 K. Devi and P. Awasthi, *J. Biomol. Struct. Dyn.*, 2021, **1**, DOI: 10.1080/07391102.2021.1893818.
- 42 R. F. Graceff, A. A. Boezio, J. Able, S. Altmann, L. M. Berry, C. Boezio, J. R. Butler, M. Chu-Moyer, M. Cooke, E. F. DiMauro, T. A. Dineen, E. F. Bojic, R. S. Foti, R. T. Fremeau, A. Guzman-Perez, H. Gao, H. Gunaydin, H. Huang, L. Huang, C. Ilch, M. Jarosh, T. Kornecook, C. R. Kreiman, D. S. La, J. Ligutti, B. C. Milgram, M. H. Jasmine Lin, I. E. Marx, H. N. Nguyen, E. A. Peterson, G. Rescouri, J. Roberts, L. Schenkel, R. Shimanovich, B. A. Sparling, J. Stellwagen, K. Taborn, K. R. Vaida, J. Wang, J. Yeoman, V. Yu, D. Zhu, B. D. Moyer and M. M. Weiss, *J. Med. Chem.*, 2017, **60**, 5990.
- 43 R. Lavanya, *Int. J. Pharm. Sci. Invent.*, 2017, **6**, 1.
- 44 M. X. Song and X. Q. Deng, *J. Enzyme Inhib. Med. Chem.*, 2018, **33**, 453.
- 45 J. R. Johansson, T. Beke-Somfai, A. Said Stålsmeden and N. Kann, *Chem. Rev.*, 2016, **116**, 14726.
- 46 Z. Xu, S. J. Zhao and Y. Liu, *Eur. J. Med. Chem.*, 2019, **183**, 111700.
- 47 J. P. Wan, S. Cao and Y. Liu, *J. Org. Chem.*, 2015, **80**, 9028.
- 48 E. Tasca, G. La Sorella, L. Sporni, G. Strukul and A. Scarso, *Green Chem.*, 2015, **17**, 1414.
- 49 X. Xu, Y. Zhong, Q. Xing, Z. Gao, J. Gou and B. Yu, *Org. Lett.*, 2020, **22**, 5176.
- 50 H. N. Liu, H. Q. Cao, C. W. Cheung and J. A. Ma, *Org. Lett.*, 2020, **22**, 1396.
- 51 X. M. Chu, C. Wang, W. L. Wang, L. L. Liang, W. Liu, K. K. Gong and K. L. Sun, *Eur. J. Med. Chem.*, 2019, **166**, 206.
- 52 B. Zhang, *Eur. J. Med. Chem.*, 2019, **168**, 357.
- 53 S. Murugavel, C. Ravikumar, G. Jaabil and P. Alagusundaram, *Comput. Biol. Chem.*, 2019, **79**, 73.
- 54 N. Batra, V. Rajendran, D. Agarwal, I. Wadi, P. C. Ghosh, R. D. Gupta and M. Nath, *ChemistrySelect*, 2018, **3**, 9790.
- 55 S. Rajan, S. Puri, D. Kumar, M. H. Babu, K. Shankar, S. Varshney, A. Srivastava, A. Gupta, M. SridharReddy and A. N. Gaikwad, *Eur. J. Med. Chem.*, 2018, **143**, 1345.
- 56 S. Vanaparthi, R. Bantu, N. Jain, S. Janardhan and L. Nagarapu, *Bioorg. Med. Chem. Lett.*, 2020, **30**, 127304.
- 57 (a) F. Karimi, M. Yarie and M. A. Zolfigol, *Mol. Catal.*, 2020, **497**, 111201; (b) P. Ghasemi, M. Yarie, M. A. Zolfigol, A. Taherpour and M. Torabi, *ACS Omega*, 2020, **5**, 3207; (c) F. Karimi, M. Yarie and M. A. Zolfigol, *RSC Adv.*, 2020, **10**, 25828; (d) F. Karimi, M. Yarie and M. A. Zolfigol, *Mol. Catal.*, 2019, **463**, 20; (e) M. Torabi, M. Yarie, M. A. Zolfigol, S. Rouhani, S. Azizi, T. O. Olomola, M. Maaza and T. A. M. Msagati, *RSC Adv.*, 2020, **11**, 3143.
- 58 (a) M. Yarie, *Iran. J. Catal.*, 2017, **7**, 85; (b) M. Yarie, *Iran. J. Catal.*, 2020, **10**, 79; (c) J. Afsar, M. A. Zolfigol, A. Khazaei, M. Zarei, Y. Gu, D. A. Alonso and A. Khoshnood, *Mol. Catal.*, 2020, **482**, 110666; (d) S. Kalhor, M. Yarie, M. Torabi, M. A. Zolfigol, M. Rezaeivala and Y. Gu, *Polycyclic Aromat. Compd.*, 2021, **11**, 17456; (e) M. Torabi, M. A. Zolfigol, M. Yarie, B. Notash, S. Azizian and M. M. Azandaryani, *Sci. Rep.*, 2021, **11**, 16846; (f) S. Kalhor, M. Zarei, M. A. Zolfigol, H. Sepehrmansourie, D. Nematollahi, S. Alizadeh, H. Shi and J. Arjomandi, *Sci. Rep.*, 2021, **11**, 19370.
- 59 (a) I. V. Alabugin, L. Kuhn, M. G. Medvedev, N. V. Krivoshchapov, V. A. Vil, I. A. Yaremenko, P. Mehaffy, M. Yarie, A. O. Terent'ev and M. A. Zolfigol, *Chem. Soc. Rev.*, 2021, **50**, 10253; (b) I. V. Alabugin, L. Kuhn, N. V. Krivoshchapov, P. Mehaffy and M. G. Medvedev, *Chem. Soc. Rev.*, 2021, **50**, 10212.
- 60 A. C. Boukis, K. Reiter, M. Frölich, D. Hofheinz and M. A. Meier, *Nat. Commun.*, 2018, **9**, 1439.
- 61 B. B. Toure and D. G. Hall, *Chem. Rev.*, 2009, **109**, 4439.
- 62 N. Isambert, M. D. M. S. Duque, J. C. Plaquevent, Y. Genisson, J. Rodriguez and T. Constantieux, *Chem. Soc. Rev.*, 2011, **40**, 1347.
- 63 M. A. Zolfigol, *Tetrahedron*, 2001, **57**, 9509.
- 64 S. Zeghada, G. Bentabed-Ababsa, A. Derdour, S. Abdelmounim, L. R. Domingo, J. A. Sáez, T. Roisnel, E. Nassar and F. Mongin, *Org. Biomol. Chem.*, 2011, **9**, 4295.

